Bound states resulting from interaction of the non-relativistic particles with the multiparameter potential

Ahmet Taş[†] and Ali Havare

Mersin University, Department of Physics, Mersin 33343, *Turkey*

(Received 19 May 2017; revised manuscript received 30 June 2017; published online 10 September 2017)

In this study, we present the analytical solutions of bound states for the Schrödinger equation with the multiparameter potential containing the different types of physical potentials via the asymptotic iteration method by applying the Pekeris-type approximation to the centrifugal potential. For any n and l (states) quantum numbers, we derive the relation that gives the energy eigenvalues for the bound states numerically and the corresponding normalized eigenfunctions. We also plot some graphics in order to investigate effects of the multiparameter potential parameters on the energy eigenvalues. Furthermore, we compare our results with the ones obtained in previous works and it is seen that our numerical results are in good agreement with the literature.

Keywords: multiparameter potential, Schrödinger equation, bound states, asymptotic iteration method

PACS: 03.65.Nk, 03.65.Ge, 02.30.Gp, 21.60.–n **DOI:** 10.1088/1674-1056/26/10/100301

1. Introduction

One of the most important tasks discussed in physics is to obtain the exact analytical solutions, which describe the bound and scattering states, of radial Schrödinger equation with arbitrary angular quantum numbers ($l = 0$ and $l \neq 0$) for various potentials.[1–16] For the s-wave states (the case of $l = 0$), the analytical solutions for the bound states can be achieved directly. On the other hand, for the l-wave states (the case of $l \neq 0$), it is necessary to use a convenient approximation to the centrifugal term ($l(l+1)/r^2$) such as the Pekeris approximation[17] and the approximation scheme proposed by Greene and Aldrich.[18] In order to obtain the relation for the energy eigenvalues which is used to get numerical results of the bound states, one needs to solve the second order differential equations. There are many solution methods of the differential equations. Some of these are the standard method,[19–21] the Nikiforov–Uvarov method (NU),[22–24] the supersymmetric shape invariance method (SUSY),[25–29] and the asymptotic iteration method (AIM).[30,31]

Some of the potentials can be generalized to explain the interactions consisting of more than one process.[32–36] Therefore, in our study, we introduce the multiparameter potential which can be used to describe the interactions in the nuclei and structures of the diatomic and polyatomic molecules, in the following form:

$$V(r) = \frac{A + B\,\mathrm{e}^{-b(r-L)}}{q + p\ \mathrm{e}^{-b(r-L)}} + \frac{C\,\mathrm{e}^{-b(r-L)} + D\,\mathrm{e}^{-2b(r-L)}}{(q + p\ \mathrm{e}^{-b(r-L)})^2}. \quad (1)$$

All of the parameters in the potential are real. The shape of the potential changes according to values of the parameters. In special cases, the multiparameter potential is reduced to potentials that have many applications in the relativistic and non-relativistic quantum mechanics such as the Manning–Rosen,[37] Hulthen,[38] Eckart-type,[39] Rosen–Morse,[40] Woods–Saxon,[41] Morse,[42] Kratzer–Fues,[43] q-parameter hyperbolic Pöschl–Teller,[44] and Yukawa[45] potentials.

The content of this study is regulated as follows: in the next section, the asymptotic iteration method is presented. In Section 3, analytical solutions for the bound states of the radial Schrödinger equation with the multiparameter potential is obtained within the framework AIM. Also in same section, for any n and l quantum numbers, the relation for energy eigenvalues is derived in a closed form and normalized eigenfunctions are obtained in terms of the hypergeometric functions by using the normalization condition of the wave functions. The special potentials which are obtained from the multiparameter potential are acquainted in Section 4 and calculated the energy eigenvalues of bound state energy eigenvalues for these potentials numerically. Finally, we discuss the results in Section 5.

2. Asymptotic iteration method

The asymptotic iteration method has been suggested to solve the homogenous linear second-order differential equation which must be in the following form[46]

$$y''(x) = \lambda_0(x)y'(x) + S_0(x)y(x), \quad (2)$$

where $\lambda_0 \neq 0$. The $S_0(x)$ and $\lambda_0(x)$ are sufficiently differentiable with respect to x. To obtain a general solution for this equation, the following procedure is supposed.

We differentiate Eq. (2) with respect to x, we obtain

$$y'''(x) = \lambda_1(x)y'(x) + S_1(x)y(x), \quad (3)$$

[†]Corresponding author. E-mail: aahmet.tas@gmail.com

© 2017 Chinese Physical Society and IOP Publishing Ltd

where

$$\lambda_1 = \lambda_0'(x) + \lambda_0(x)\lambda_0(x) + S_0(x),$$
$$S_1(x) = S_0'(x) + S_0(x)\lambda_0(x). \tag{4}$$

The second derivative of Eq. (2) becomes

$$y^{(iv)}(x) = \lambda_2(x)y'(x) + S_2(x)y(x), \tag{5}$$

where

$$\lambda_2 = \lambda_1'(x) + \lambda_0(x)\lambda_1(x) + S_1(x),$$
$$S_2(x) = S_0(x)\lambda_1(x) + S_1'(x). \tag{6}$$

Finally, by taking $(k+1)$-th and $(k+2)$-th derivative of Eq. (2), $k = 1, 2, 3, \ldots$, we find the following equations respectively

$$y^{(k+1)}(x) = \lambda_{k-1}(x)y'(x) + S_{k-1}(x)y(x),$$
$$y^{(k+2)}(x) = \lambda_k(x)y'(x) + S_k(x)y(x), \tag{7}$$

where

$$\lambda_{k-1} = \lambda_{k-2}'(x) + \lambda_0(x)\lambda_{k-2}(x) + S_{k-2}(x),$$
$$S_{k-1}(x) = S_0(x)\lambda_{k-2}(x) + S_{k-2}'(x),$$
$$\lambda_k = \lambda_{k-1}'(x) + \lambda_0(x)\lambda_{k-1}(x) + S_{k-1}(x),$$
$$S_k(x) = S_0(x)\lambda_{k-1}(x) + S_{k-1}'(x). \tag{8}$$

Therefore, from Eq. (7) we can obtain the following relation

$$\frac{y^{(k+2)}(x)}{y^{(k+1)}(x)} = \frac{\lambda_k\left[y'(x) + \frac{S_k(x)}{\lambda_k(x)}y(x)\right]}{\lambda_{k-1}\left[y'(x) + \frac{S_{k-1}}{\lambda_{k-1}}y(x)\right]}. \tag{9}$$

For sufficiently large value of k, if

$$\frac{S_k(x)}{\lambda_k(x)} = \frac{S_{k-1}(x)}{\lambda_{k-1}(x)} = \cdots = \alpha(x), \tag{10}$$

which is the "asymptotic" aspect of the method, in that case, equation (9) reduces to

$$\frac{\mathrm{d}}{\mathrm{d}x}\ln\left[y^{(k+1)(x)}\right] = \frac{\lambda_k(x)}{\lambda_{k-1}(x}, \tag{11}$$

which leads to the general solution of Eq. (2) as

$$y(x) = \exp\left\{\int^x \left[\lambda_0(x') + \alpha(x')\right]\mathrm{d}x'\right\} \cdot \left[C_2 + C_1\int^x \exp\left\{\int^{x'}\left[\lambda_0(x'') + \alpha(x'')\right]\mathrm{d}x''\right\}\mathrm{d}x'\right], \tag{12}$$

where C_1 and C_2 are integration constants. For any given potential, the radial part of the Schrödinger equation is transformed into the form of Eq. (2). Then, the $\lambda_0(x)$ and $S_0(x)$ coefficients are found and $\lambda_k(x)$ and $S_k(x)$ parameters are calculated by using recurrence relations defined by Eq. (8). Then, taking into account the condition given by Eq. (10), the energy eigenvalues are obtained if the problem is the exactly solvable. Equation (10) can be expressed in the following manner:

$$\delta_k(x) = \lambda_k(x)S_{k-1}(x) - \lambda_{k-1}(x)S_k(x), \quad k = 1, 2, 3, \ldots \tag{13}$$

We want to obtain the exact solutions of the radial Schrödinger equation for which the relevant second order homogenous linear differential equation takes the following general form[47]

$$y''(x) = 2\left[\frac{ax^{N+1}}{1 - bx^{N+2}} - \frac{(t+1)}{x}\right]y'(x) - \frac{Wx^N}{1 - bx^{N+2}}y(x). \tag{14}$$

The exact solutions for this equation are given by

$$y_n(x) = (-1)^n C(N+2)^n(\sigma)_n\, {}_2\mathrm{F}_1(-n,\ \rho + n;\ \sigma;\ bx^{N+2}), \tag{15}$$

where

$$(\sigma)_n = \frac{\Gamma(\sigma + n)}{\sigma}, \quad \sigma = \frac{2t + N + 3}{N + 2},$$
$$\rho = \frac{(2t+1)b + 2a}{(N+2)b}. \tag{16}$$

The energy eigenfunctions can be obtained by using Eq. (14) directly.

3. Bound state solutions of the Schrödinger equation: Calculation of the energy eigenvalues and eigenfunctions

The Schrödinger equation in spherical coordinate for a particle with energy E moving in a external potential is written as the following form (in natural units $\hbar = m = 1$):

$$\left[-\frac{1}{2}\nabla^2 + V(r) - E\right]\psi_{nlm}(r, \theta, \phi) = 0. \tag{17}$$

If the wave function is selected as

$$\psi_{nlm}(r, \theta, \phi) = r^{-1}R_{nl}(r)\,\mathrm{Y}_{lm}(\theta, \phi)$$

and the necessary calculations are done, the radial part of the Schrödinger equaiton is obtained as the following form

$$\frac{\mathrm{d}^2R_{nl}}{\mathrm{d}r^2} + \left\{2\left[E - V(r)\right] - \frac{l(l+1)}{r^2}\right\}R_{nl} = 0. \tag{18}$$

Substituting Eq. (1) into Eq. (18) gives,

$$\frac{\mathrm{d}^2R_{nl}}{\mathrm{d}r^2} + \left\{2\left[E - \frac{A + B\,\mathrm{e}^{-b(r-L)}}{q + p\ \mathrm{e}^{-b(r-L)}} - \frac{C\,\mathrm{e}^{-b(r-L)} + D\,\mathrm{e}^{-2b(r-L)}}{(q + p\ \mathrm{e}^{-b(r-L)})^2}\right] - \frac{l(l+1)}{r^2}\right\}R_{nl} = 0. \tag{19}$$

To find the analytical solutions of this equation we must use the following approximation which is called the Pekeris approximation.[48] This approximation is applied to the centrifugal term

$$\frac{1}{r^2} \approx C_0 + \frac{C_1}{p+q\,\mathrm{e}^{b(r-L)}} + \frac{C_2}{(p+q\,\mathrm{e}^{b(r-L)})^2}, \tag{20}$$

where C_0, C_1 and C_2 are constants and their values are calculated by expanding the terms in Eq. (20) as follows:

$$C_0 = \frac{(3+bL)p^2 - 2(-3+bL)pq + (3-3bL+b^2L^2)q^2}{b^2q^2L^4},$$

$$C_1 = \frac{2(p+q)^2\left[(3+bL)p+(3-2bL)q\right]}{b^2q^2L^4},$$

$$C_2 = \frac{(p+q)^3\left[(3+bL)p+(3-bL)q\right]}{b^2q^2L^4}. \tag{21}$$

The terms in Eq. (20) are expanded in a series about $r \approx L$ because the nuclear distance r does not fluctuate very far from the equilibrium position at L.[49] Therefore the approximation in Eq. (20) gives good result only for $r \approx L$. Substituting Eq. (20) into Eq. (19), we obtain

$$\frac{\mathrm{d}^2R_{nl}}{\mathrm{d}r^2} + \left[\varepsilon_1 - \frac{\varepsilon_2+\varepsilon_3}{q+p\,\mathrm{e}^{-b(r-L)}} + \frac{\varepsilon_4\,\mathrm{e}^{-b(r-L)} + \varepsilon_5\,\mathrm{e}^{-2b(r-L)}}{(q+p\,\mathrm{e}^{-b(r-L)})^2}\right] R_{nl} = 0, \tag{22}$$

where the parameters ε_1, ε_2, ε_3, ε_4, and ε_5 are defined as follows:

$$\varepsilon_1 = 2E - l(l+1)C_0, \quad \varepsilon_2 = 2A, \quad \varepsilon_3 = 2B - l(l+1)C_1, \quad \varepsilon_4 = 2C, \quad \varepsilon_5 = 2D - l(l+1)C_2. \tag{23}$$

If we use a new variable $y = p/(p+q\,\mathrm{e}^{b(r-L)})$ in Eq. (22) we obtain the following equation:

$$y(1-y)\frac{\mathrm{d}^2R_{nl}}{\mathrm{d}y^2} + (1-2y)\frac{\mathrm{d}R_{nl}}{\mathrm{d}y} + \frac{1}{y(1-y)}\left[-\alpha^2 - \beta y - \gamma y^2\right] R_{nl} = 0, \tag{24}$$

where

$$\alpha^2 = \frac{1}{b^2}\left[\frac{\varepsilon_2}{q} - \varepsilon_1\right], \quad \beta = \frac{1}{b^2}\left[\frac{\varepsilon_3}{p} + \frac{\varepsilon_4}{pq} - \frac{\varepsilon_2}{q}\right], \quad \gamma = \frac{1}{b^2}\left[\frac{\varepsilon_5}{p^2} + \frac{\varepsilon_4}{pq}\right]. \tag{25}$$

Note that equation (24) has second degree singular pole points at $y = 0$ and $y = 1$. In order to remove these singularities and get a solution for Eq. (24) with AIM, we write the reasonable physical wave functions as follows:

$$R_{nl}(y) = y^{\alpha}(1-y)^{\sqrt{\alpha^2+\beta+\gamma}} f_{nl}(y), \tag{26}$$

with boundary conditions

$$R_{nl}(r) = \begin{cases} 0, & r \to \infty\ (y=0), \\ 0, & r \to 0\ (y \approx 1). \end{cases}$$

We use the $b \cdot L \gg 1$ approximation here in order to ensure the boundary conditions of wave functions. If $b \cdot L \gg 1$, $\mathrm{e}^{-bL} \approx 0$ and then $y \approx 1$. By substituting Eq. (26) into Eq. (24), we obtain the second-order homogeneous equation which is compatible with Eq. (2)

$$\frac{\mathrm{d}^2f_{nl}}{\mathrm{d}y^2} = \left[\frac{\left(2\alpha+2\sqrt{\alpha^2+\beta+\gamma}+2\right)y-(1+2\alpha)}{y(1-y)}\right]\frac{\mathrm{d}f_{nl}}{\mathrm{d}y} + \left[\frac{\beta+2\alpha\sqrt{\alpha^2+\beta+\gamma}+2\alpha^2+\alpha+\sqrt{\alpha^2+\beta+\gamma}}{y(1-y)}\right] f_{nl}. \tag{27}$$

Now we can use the AIM to solve this equation, comparing Eq. (27) with Eq. (2) and using the recurrence relations which are defined in Eq. (8), one obtains the values of λ_n and S_n as follows:

$$\begin{aligned}
\lambda_0(y) &= \frac{\left(2\alpha+2\sqrt{\alpha^2+\beta+\gamma}+2\right)y-(1+2\alpha)}{y(1-y)}, \\
S_0(y) &= \frac{\beta+2\alpha\sqrt{\alpha^2+\beta+\gamma}+2\alpha^2+\alpha+\sqrt{\alpha^2+\beta+\gamma}}{y(1-y)}, \\
\lambda_1(y) &= \frac{1}{(y-1)^2y^2}\left\{2+6\alpha+4\alpha^2+y^2\left[6+3\beta+4\gamma+9\sqrt{\alpha^2+\beta+\gamma}+3\alpha\left(3+2\alpha+2\sqrt{\alpha^2+\beta+\gamma}\right)\right]\right. \\
&\quad \left. -y\left[6-\beta+3\sqrt{\alpha^2+\beta+\gamma}+3\alpha\left(5+2\alpha+2\sqrt{\alpha^2+\beta+\gamma}\right)\right]\right\}, \\
S_1(y) &= \frac{1}{(y-1)^2y^2}2\left[\alpha+2\alpha^2+\beta+2\alpha\sqrt{\alpha^2+\beta+\gamma}\right]\left[-1-\alpha+y\left(2+\alpha+\sqrt{\alpha^2+\beta+\gamma}\right)\right], \\
&\cdots
\end{aligned} \tag{28}$$

If we write the above equations into the condition defined in Eq. (13), we acquire

$$\alpha_0 = -\frac{\beta+2\gamma-\sqrt{\beta^2(1+4\gamma)}}{4\gamma}, \quad \alpha_1 = -\frac{6-3\beta-6\gamma+\sqrt{(2+\beta)^2(1+4\gamma)}}{4(\gamma-2)},$$
$$\alpha_2 = -\frac{30-5\beta-10\gamma+\sqrt{(6+\beta)^2(1+4\gamma)}}{4(\gamma-6)}, \quad \ldots, \tag{29}$$

with the generalization of these relations

$$\alpha_n = -\frac{1}{4(\gamma-n(n-1))}\left[(1+2n)(n+n^2-\beta-2\gamma)+\sqrt{(n+n^2+\beta^2)(1+4\gamma)}\right]. \tag{30}$$

Then, by using notations (25), the energy eigenvalues of the Schrödinger equation with the multiparameter potential is obtained as follows:

$$E_{nl} = \frac{1}{2}\left\{\frac{\varepsilon_2}{q}+l(l+1)C_0-b^2\alpha_n^2\right\}. \tag{31}$$

By using this relation, the energy eigenvalues can be calculated for any n and l quantum numbers. The energy values obtained for some values given in the parameters are presented in Table 1.

Table 1. The bound state energy eigenvalues for the multiparameter potential for $A=-5$ fm^{-1}, $B=2$ fm^{-1}, $C=1$ fm^{-1}, $D=1$ fm^{-1}, $p=1.5$, $q=3.5$, $b=2$ fm^{-1}, and $L=7$ fm in atomic units $\hbar=m=1$.

n	l	States	E_{nl}	n	l	States	E_{nl}
1	0	1s	−1.48143	5	1	5p	−8.33271
2	0	2s	−2.34743	5	2	5d	−4.72222
2	1	2p	−1.46934	5	3	5f	−2.20381
3	0	3s	−4.80639	5	4	5g	−1.36711
3	1	3p	−2.32348	6	0	6s	−18.5502
3	2	3d	−1.44558	6	1	6p	−12.9172
4	0	4s	−8.36378	6	2	6d	−8.27048
4	1	4p	−4.77835	6	3	6f	−4.63788
4	2	4d	−2.27559	6	4	6g	−2.10820
4	3	4f	−1.41103	6	5	6h	−1.31591
5	0	5s	−12.9510	7	0	7s	−25.1552

Let us now obtain the wave functions. By comparing Eq. (27) with Eq. (14), we obtain

$$N=-1, \qquad b=1, \qquad a=\frac{2\nu+1}{2},$$
$$t=\frac{2\mu-1}{2}, \qquad w=2\mu^2+2\mu\nu+\beta, \tag{32}$$

where $\mu=\alpha$ and $\nu=\sqrt{\alpha^2+\beta+\gamma}$. Then, the wave function $(f_{nl}(y))$ yields

$$f_{nl}(y) = (-1)^n\, C\, (\sigma)_n\, {}_2F_1(-n,\rho+n;\sigma;y), \tag{33}$$

where

$$\sigma = 2\mu+1, \qquad (\sigma)_n = \frac{\Gamma(2\mu+n+1)}{2\mu+1},$$
$$\rho = 2\mu+2\nu+1. \tag{34}$$

By using Eq. (26), Eq. (33) and Eq. (34), the total radial wave functions of the Schrödinger equation with the multiparameter potential can be written as the following form

$$R_{nl}(y) = C_{nl}\,(-1)^n y^{\mu}(1-y)^{\nu}\left[\frac{\Gamma(2\mu+n+1)}{2\mu+1}\right] \cdot {}_2F_1(-n,n+2\mu+2\nu+1;2\mu+1;y), \tag{35}$$

where ${}_2F_1$ is the Gauss hypergeometric function and C_{nl} is the normalization constant and it can be calculated by using the normalization condition of the wave function. Then, we obtain

$$\int_0^{\infty}|R_{nl}(r)|^2\,\mathrm{d}r = \frac{1}{b}\int_0^1\frac{(1-y)}{y}|R_{nl}(y)|^2\,\mathrm{d}y = 1. \tag{36}$$

If we replace Eq. (35) with the above equation, we obtain

$$\frac{|C_{nl}|^2}{b}\left(\frac{\Gamma(2\mu+n+1)}{2\mu+1}\right)^2\int_0^1 y^{2\mu-1}(1-y)^{2\nu+1}\left[{}_2F_1(-n,n+2\mu+2\nu+1;1+2\mu;y)\right]^2\mathrm{d}y = 1. \tag{37}$$

The integral in Eq. (37) is calculated for different n values using the Mathematica software program for $\mathrm{Re}\,|\mu|>0$ and $\mathrm{Re}\,|\nu|>-1$ as follows:

$$\frac{\Gamma(2\mu)\Gamma(2+2\nu)}{\Gamma(2+2\mu+2\nu)} \quad \text{for} \quad n=0,$$
$$\frac{(3+2\nu)}{2\mu(3+2\mu+2\nu)(1+2\mu)^2}\frac{\Gamma(2+2\mu)\Gamma(2+2\nu)}{\Gamma(2+2\mu+2\nu)} \quad \text{for} \quad n=1,$$
$$\frac{(5+2\nu)}{4\mu(5+2\mu+2\nu)(1+3\mu+2\mu^2)^2}\frac{\Gamma(3+2\mu)\Gamma(3+2\nu)}{\Gamma(3+2\mu+2\nu)} \quad \text{for} \quad n=2,$$

$$\frac{3(7+2\nu)}{4\mu(7+2\mu+2\nu)(3+11\mu+12\mu^2+4\mu^3)^2}\frac{\Gamma(4+2\mu)\Gamma(4+2\nu)}{\Gamma(4+2\mu+2\nu)} \quad \text{for} \quad n=3,$$
$$\frac{m!(2\nu+2m+1)}{(2\mu+2\nu+2m+1)}\frac{\Gamma(2\mu+1)\Gamma(2\nu+2m+1)}{\Gamma(2\mu+m+1)\Gamma(2\mu+2\nu+2m+1)} \quad \text{for} \quad n=m. \tag{38}$$

Therefore, we achieve

$$C_{nl}=\sqrt{\frac{b\,(2\mu+1)^2(2\mu+2\nu+2n+1)\Gamma(2\mu+2\nu+2n+1)}{n!(\nu+2n+1)\Gamma(2\mu+1)\Gamma(2\nu+2n+1)\Gamma(2\mu+n+1)}}. \tag{39}$$

4. Numerical results for the special cases

The potentials that have many applications in the quantum mechanics can be obtained from the multiparameter potential under the certain conditions. For some of these potentials, the energy eigenvalues are calculated and compared with data obtained in earlier studies. On the other hand, there are no numerical results in the literature for some potentials, so the numerical values given to the parameters are chosen in this study and the energy eigenvalues obtained cannot been compared.

Potential-type 1: The Manning–Rosen potential

For $A=C=0$, $B=-K/2m\beta^2$, $D=\alpha(\alpha-1)/2m\beta^2$, $q=\mathrm{e}^{bL}$, $p=-1$, and $b=1/\beta$, the multiparameter potential is turned into the Mannig–Rosen potential as follows:

$$V_{M-R}(r)=\frac{1}{2m\beta^2}\left[\frac{\alpha(\alpha-1)\,\mathrm{e}^{-2r/\beta}}{(1-\mathrm{e}^{-2r/\beta})^2}-\frac{K\,\mathrm{e}^{-r/\beta}}{1-\mathrm{e}^{-2r/\beta}}\right], \tag{40}$$

where α and K are two dimensionless parameters, parameter β is related to the range of the potential and has dimension of length.[50] By using Eq. (31), the energy eigenvalues of the Manning–Rosen potential are calculated. For $A=C=0$, $B=0.025$, $D=-5.8\times10^{-5}$, $p=1$, $L=5$, and different values of the parameter b, the energy values of bound state are obtained and these are shown in Table 2. By analyzing Table 2, we see that our numerical results are compatible with the results of Refs. [51]–[54].

Table 2. Energy eigenvalues for the Manning–Rosen potential, which is obtained from the multiparameter potential, in atomic units for $\hbar=1$ and $m=1$.

States	$1/b$	E_{nl}	E_{nl}[51]	E_{nl}[52]	E_{nl}[53]	E_{nl}[54]
	0.025	−0.1205270	−0.120527265	−0.1205271	−0.1205270	−0.1205793
2p	0.050	−0.1082150	−0.108214465	−0.1082151	−0.1082140	−0.1084228
	0.075	−0.0964429	−0.096443282	−0.0964469	−0.0964433	−0.0969120
	0.025	−0.0458778	−0.045877611	−0.0458779	−0.0458776	−0.0459296
3p	0.050	−0.0350593	−0.035058868	−0.0350633	−0.0035058	−0.0352672
	0.075	−0.0255467	−0.025542209	−0.0255654	−0.0255422	−0.0260109
	0.025	−0.0447740	−0.044773693	−0.0447743	−0.0447737	−0.0449299
3d	0.050	−0.0336846	−0.033683244	−0.0336930	−0.0336832	−0.0343082
	0.075	−0.0237299	−0.023710563	−0.0237621	−0.0237106	−0.0251168
4p	0.025	−0.0208089	−0.020808737	−0.0208097	−0.0208087	−0.0208608
	0.050	−0.0117214	−0.011720853	−0.0117365	−0.0117209	−0.0119291
4d	0.025	−0.0202998	−0.020299297	−0.0203017	−0.0202993	−0.0204555
	0.050	−0.0109507	−0.010949158	−0.0109904	−0.0109492	−0.0115741
4f	0.025	−0.0199771	−0.019976163	−0.0199797	−0.0199762	−0.0202886
	0.050	−0.0101815	−0.010178355	−0.0102393	−0.0101784	−0.0114283
5p	0.025	−0.0098057	−0.009805520	−0.0098079	−0.0098055	−0.0098576
5d	0.025	−0.0095080	−0.009507438	−0.0095141	−0.0095074	−0.0096637
5f	0.025	−0.0092722	−0.009271176	−0.0092825	−0.0092712	−0.0095837
5g	0.025	−0.0090208	−0.009018988	−0.0090330	−0.0090190	−0.0095398
6p	0.025	−0.0043532	−0.004149868	−0.0043583	−0.0043531	−0.0044051
6d	0.025	−0.0041504	−0.003952747	−0.0041650	−0.0041499	−0.0043061
6f	0.025	−0.0039539	−0.003722009	−0.0039803	−0.0039528	−0.0042652
6g	0.025	−0.0037240	−0.003722009	−0.0037611	−0.0037220	−0.0042428

Potential-type 2: The Hulthen potential

If the parameters of Eq. (1) are arranged as $A=C=D=0$, $B=-V_0$, $q=\mathrm{e}^{bL}$, $p=-1$, and $b=2\alpha$, the equation (1) reduces to the Hulthen potential:

$$V_H(r)=-V_0\frac{\mathrm{e}^{-2\alpha r}}{1-\mathrm{e}^{-2\alpha r}}. \tag{41}$$

The energy eigenvalues for the bound state of the Hulthen Potential are calculated for $A = C = D = 0$, $B = -0.025$, $p = -1$, $L = 5$, and different values of the parameter b by using Eq. (31) and these are also presented in Table 3. By testing Table 3, ones can see that our numerical results are consistent with the results of Refs. [55]–[58].

Table 3. Energy eigenvalues for the Hulthen potential, which is obtained from the multiparameter potential, in atomic units for $\hbar = 1$ and $m = 1$.

States	b	E_{nl}	E_{nl} [55]	E_{nl} [56]	E_{nl} [57]	E_{nl} [58]
2p	0.025	−0.112761	−0.1128125	−0.1128125	−0.1127605	−0.1127605
	0.050	−0.101043	−0.1012500	−0.1012500	−0.1010425	−0.1010425
	0.075	−0.0898511	−0.0903125	−0.0903125	−0.0898478	−0.0898478
3p	0.025	−0.0437067	−0.0437590	−0.0437590	−0.0437068	−0.0437069
	0.050	−0.0331619	−0.0333681	−0.0333681	−0.0331632	−0.0331645
	0.075	−0.023926	−0.0243837	−0.0243837	−0.0239331	−0.0239397
3d	0.025	−0.0436028	−0.0437587	−0.0437587	−0.0436030	−0.0436030
	0.050	−0.0327483	−0.0333681	−0.0333681	−0.0327532	−0.0327532
	0.075	−0.0230042	−0.0243837	−0.0243837	−0.0230306	−0.0230307
4p	0.025	−0.0199481	−0.0200000	−0.0200000	−0.0199480	−0.0199489
	0.050	−0.0110444	−0.0112500	−0.0112500	−0.0110430	−0.0110582
4d	0.025	−0.0198442	−0.0200000	−0.0200000	−0.0198460	−0.0198462
	0.050	−0.0106328	−0.0112500	−0.0112500	−0.0106609	−0.0106674
4f	0.025	−0.0196884	−0.0200000	−0.0200000	−0.0196911	−0.0196911
	0.050	−0.0100151	−0.0112500	−0.0112500	−0.0100618	−0.0100620
5p	0.025	−0.00940124	−0.0094531	−0.0094531	−0.0094011	−0.0094036
5d	0.025	−0.00929744	−0.0094531	−0.0094531	−0.0092977	−0.0093037
5f	0.025	−0.00914174	−0.0094531	−0.0094531	−0.0091507	−0.0091521
5g	0.025	−0.00893414	−0.0094531	−0.0094531	−0.0089465	−0.0089465
6p	0.025	−0.00414951	−0.0042014	−0.0042014	−0.0041493	−0.0041548
6d	0.025	−0.00404575	−0.0042014	−0.0042014	−0.0040452	−0.0040606
6f	0.025	−0.00389011	−0.0042014	−0.0042014	−0.0038901	−0.0039168
6g	0.025	−0.00368258	−0.0042014	−0.0042014	−0.0036943	−0.0037201

Potential-type 3: The Eckart-type potential

By taking $A = D = 0$, $B = -\alpha$, $C = \beta\, \mathrm{e}^{bL}$, $q = \mathrm{e}^{bL}$, $p = 1$, and $b = 1/a$ in Eq. (1), the Eckart-type potential can be obtained as follows:

$$V_E(r) = -\alpha \frac{\mathrm{e}^{-r/a}}{1 - \mathrm{e}^{-r/a}} + \beta \frac{\mathrm{e}^{-r/a}}{(1 - \mathrm{e}^{-r/a})^2}. \tag{42}$$

For $A = D = 0$, $B = -0.025$, $C = 5.38 \times 10^{-5}$, $p = -1$, $L = 3$, and different values of the parameter b, the energy values of the Eckart-type potential are found by using Eq. (31). The numerical results are given in Table 4. By analyzing Table 4, we see that our numerical results are compatible with the results of Refs. [52], [59], and [60].

Table 4. Energy eigenvalues for the Eckart-type potential, which is obtained from the multiparameter potential, in atomic units for $\hbar = 1$ and $m = 1$.

States	b	E_{nl}	E_{nl} [52]	E_{nl} [59]	E_{nl} [60]
2p	0.025	−0.106474	−0.1064737	−0.106525783	−0.111363
	0.050	−0.0994941	−0.0994162	−0.099623699	−0.100968
	0.075	−0.0890665	−0.0891284	−0.089593142	−0.090161
3p	0.025	−0.0418398	−0.0418400	−0.041891799	−0.043284
	0.050	−0.0326972	−0.0327011	−0.032904593	−0.033267
	0.075	−0.0237016	−0.0237464	−0.024190255	−0.024332
3d	0.025	−0.0424583	−0.0424588	−0.042614432	−0.043407
	0.050	−0.032466	−0.0324736	−0.033088405	−0.033274
	0.075	−0.0228493	−0.0229146	−0.024267318	−0.024333
4p	0.025	−0.0191778	−0.0191787	−0.019229775	−0.0197893
	0.050	−0.0108696	−0.0108852	−0.011076854	−0.0112070

Table 4. (continued)

States	b	E_{nl}	E_{nl} [52]	E_{nl} [59]	E_{nl} [60]
4d	0.025	−0.0193729	−0.0193753	−0.019528975	−0.0198398
	0.050	−0.0105239	−0.0105633	−0.011145560	−0.0112098
4f	0.025	−0.0193492	−0.0193525	−0.019661314	−0.0198615
	0.050	−0.00993178	−0.0099876	−0.011175262	−0.0112110
5p	0.025	−0.00902945	−0.0090320	−0.009081454	−0.0093460
5d	0.025	−0.00907005	−0.0090768	−0.009226070	−0.0093703
5f	0.025	−0.00897789	−0.0089892	−0.009289939	−0.0093807
5g	0.025	−0.00880573	−0.0088194	−0.009325821	−0.0093866
6p	0.025	−0.00395921	−0.0039648	−0.004011215	−0.0041446
6d	0.025	−0.00392922	−0.0039447	−0.004085228	−0.0041570
6f	0.025	−0.00380588	−0.0038337	−0.004117909	−0.0041623
6g	0.025	−0.00361622	−0.0036554	−0.004136268	−0.0041653

Potential-type 4: The Rosen–Morse potential

if the parameters of Eq. (1) are organized as $A = V_2\,\mathrm{e}^{bL}$, $B = -V_2$, $C = 0$, $D = -4V_1$, $q = \mathrm{e}^{bL}$, $p = 1$, and $b = -2\alpha$, the Rosen–Morse potential is found as the following form

$$V_{R-M}(r) = -V_1\,\mathrm{sech}^2\,\alpha r + V_2 \tanh \alpha r, \tag{43}$$

where V_1 and V_2 are the depth of the potential and α is the range of the potential.[61] By taking $A = 3$, $B = -3$, $C = 0$, $D = -0.5$, $q = e^{bL}$, $p = 1$, $L = 5$, and $b = 0.025$, the energy eigenvalues are obtained by using Eq. (31). These results are presented in Table 5.

Table 5. Energy eigenvalues for Rosen–Morse (RM), Woods–Saxon (WS), Morse (M), Kratzer–Fues (KF), q-parameter hyperbolic Pöschl–Teller (q-PHP), and Yukawa (Y) potentials, which are obtained from the multiparameter potential, in atomic units for $\hbar = 1$ and $m = 1$.

States	$E_{nl}^{(\mathrm{RM})}$	$E_{nl}^{(\mathrm{WS})}$	$E_{nl}^{(\mathrm{M})}$	$E_{nl}^{(\mathrm{KF})}$	$E_{nl}^{(q-\mathrm{PHP})}$	$E_{nl}^{(\mathrm{Y})}$
2p	−0.899356	−0.915412	−0.914256	−0.1074060	−0.897825	−0.4510490
3p	−0.804291	−0.818112	−0.806093	−0.0501966	−0.795638	−0.1748290
3d	−0.717842	−0.804521	−0.835172	−0.0523069	−0.808880	−0.1744130
4p	−0.709394	−0.721438	−0.700429	−0.0289868	−0.694119	−0.0797943
4d	−0.550200	−0.635509	−0.674016	−0.0299852	−0.638900	−0.0793806
4f	−0.580086	−0.684029	−0.729810	−0.0306000	−0.694775	−0.0787592
5p	−0.614663	−0.625390	−0.597266	−0.0188622	−0.593268	−0.0376070
5d	−0.382720	−0.467122	−0.515359	−0.0194510	−0.469592	−0.0371948
5f	−0.342082	−0.444883	−0.511859	−0.0198723	−0.456842	−0.0365762
5g	−0.429659	−0.540350	−0.598584	−0.0202760	−0.554437	−0.0357511
6p	−0.520099	−0.529968	−0.496603	−0.0132550	−0.493085	−0.0166002
6d	−0.215401	−0.299361	−0.359203	−0.0136588	−0.300959	−0.0161890
6f	−0.104238	−0.206365	−0.296408	−0.0139935	−0.219585	−0.0155719
6g	−0.121931	−0.231522	−0.322358	−0.0143472	−0.248497	−0.0147490

Potential-type 5: The Woods–Saxon potential

The parameters in Eq. (1) are chosen as $A = C = D = 0$, $B = -V_0$, $q = 1$, $p = 1$, $b = 1/a$, and $L = R$, the multiparameter potential is transformed to the Woods–Saxon potential as

$$V_{\mathrm{WS}}(r) = -\frac{V_0}{1 + \mathrm{e}^{[(r-R)/a]}}, \tag{44}$$

where the parameter V_0 is the potential depth, R is the width of the potential, a is the surface thickness.[62] For $A = C = D = 0$, $B = -2$, $q = 1$, $p = 1$, $L = 5$, and $b = 0.05$, the energy values are calculated by using Eq. (31). These results are given in Table 5.

Potential-type 6: The Morse potential

Setting the parameters as $A = C = 0$, $B = -2D_e$, $D = D_e$, $q = 1$, $b = a$, and $L = r_\mathrm{e}$ additionally taking $\lim_{p\to 0}$ in Eq. (1), the Morse potential is obtained,

$$\begin{aligned} V_{\mathrm{M}}(r) &= \lim_{p\to 0}\left[\frac{D_\mathrm{e}\,\mathrm{e}^{-2a(r-r_\mathrm{e})}}{(1+p\,\mathrm{e}^{-a(r-r_\mathrm{e})})^2} - \frac{2D_\mathrm{e}\,\mathrm{e}^{-a(r-r_\mathrm{e})}}{(1+p\,\mathrm{e}^{-a(r-r_\mathrm{e})})}\right] \\ &= D_\mathrm{e}\left[\mathrm{e}^{-2a(r-r_\mathrm{e})} - 2\,\mathrm{e}^{a(r-r_\mathrm{e})}\right], \end{aligned} \tag{45}$$

where D_e is the dissociation energy, r_e is the equilibrium bond

length, and a denotes the range of the potential.[63] By using Eq. (31) for $A=0, B=-2, C=0, D=1, q=1, p=1\times10^{-9}$, $L=5$, and $b=0.05$, the energy spectra are found and these results are shown in Table 5.

Potential-type 7: Kratzer–Fues potential

Considering $A=C=0$, $B=-2D_{\rm e}r_{\rm e}b$, $D=D_{\rm e}r_{\rm e}^2b^2$, $q=\mathrm{e}^{bL}$, and $p=-1$ also taking $\lim\limits_{b\to0}$ in Eq. (1), the multiparameter potential reduces to the Kratzer–Fues potential:

$$V_{K-F}(r)=\lim_{b\to0}\left[\frac{D_{\rm e}r_{\rm e}^2b^2\,\mathrm{e}^{-2br}}{(1-\mathrm{e}^{-br})^2}-\frac{2D_{\rm e}r_{\rm e}b\,\mathrm{e}^{-br}}{(1-\mathrm{e}^{-br})}\right]$$
$$=-D_{\rm e}\left[\frac{2r_{\rm e}}{r}-\frac{r_{\rm e}^2}{r}\right]. \tag{46}$$

By using Eq. (31) and taking the parameters as $A=0$, $B=2\times10^{-7}$, $C=0$, $D=2.5\times10^{-15}$, $q=\mathrm{e}^{bL}$, $p=-1$, $L=5$, and $b=1\times10^{-7}$, the energy eigenvalues of the Kratzer–Fues potential are calculated and these results are shown in Table 5.

Potential-type 8: q-parameter hyperbolic Pöschl–Teller potential

For $A=C=0$, $B=-4V_0$, $D=4V_0$, $q=\mathrm{e}^{2\alpha L}$, $p=\tilde{q}$, and $b=2\alpha$, the multiparameter potential reduces to the q-parameter hyperbolic Pöschl–Teller potential:

$$V_{q-\rm PHP}(r)=-V_0\frac{4}{(\mathrm{e}^{\alpha r}+\tilde{q}\,\mathrm{e}^{\alpha r})^2}=\frac{V_0}{\cosh^2_{\tilde{q}}(\alpha r)}, \tag{47}$$

where q is the deformation parameter. V_0 is the height of the potential and α is the range of the potential barrier.[64,65] For $A=0, B=2\times10^{-7}, C=0, D=2.5\times10^{-15}, q=\mathrm{e}^{bL}, p=-1$, $L=5$, and $b=1\times10^{-7}$, the energy eigenvalues are obtained by using Eq. (31) and these results are given in Table 5.

Potential-type 9: Yukawa potential

Setting the parameters $A=C=0$, $B=-2\alpha V_0$, $D=0$, $q=\mathrm{e}^{bL}$, $p=-1$, and $b=2\alpha$ also using approximation $(2\alpha\,\mathrm{e}^{\alpha r}/(1-\mathrm{e}^{-2\alpha r})\approx1/r$ in Eq. (1), the Yukawa potential is obtained as the following form:

$$V_Y(r)=-V_0\,\mathrm{e}^{\alpha r}\left(\frac{2\alpha\,\mathrm{e}^{-\alpha r}}{1-\mathrm{e}^{-2\alpha r}}\right)\approx-V_0\frac{\mathrm{e}^{-\alpha r}}{r}. \tag{48}$$

The energy eigenvalues for the bound state of the Yukawa potential are calculated by using Eq. (31) for $A=0$, $B=-0.1$, $C=0$, $D=0$, $q=\mathrm{e}^{bL}$, $p=-1$, $L=5$, and $b=0.05$. These results are shown in Table 5.

5. Conclusion

In this paper, we have obtained the analytical solutions of the bound state for the Schrödinger equation with the multiparameter potential via the AIM. In order to solve the radial Schrödinger equation for $l\neq0$, the Pekeris-type approximation has been applied to the centrifugal potential. Taking into account the boundary conditions of the wave function, the relation obtained for the energy eigenvalues has been derived and by using the normalization condition for the wave functions, we have calculated the normalization constant in terms of the gamma functions. By giving appropriate values to the parameters, the energy eigenvalues for the bound states have been calculated for both $l=0$ and $l\neq0$ states numerically and are given in Table 1.

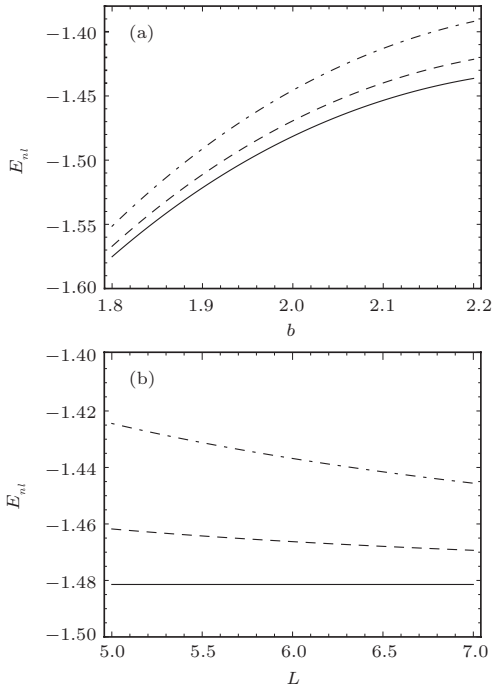


Fig. 1. The effect of parameters b and L on the energy eigenvalues. Figure 1(a) shows E_{nl} varying with b for $A=-5$ fm^{-1}, $B=2$ fm^{-1}, $C=1$ fm^{-1}, $D=1$ fm^{-1}, $p=1.5$, $q=3.5$, and $L=7$ fm. Figure 1(b) displays E_{nl} varying with L for $A=-5$ fm^{-1}, $B=2$ fm^{-1}, $C=1$ fm^{-1}, $D=1$ fm^{-1}, $p=1.5$, $q=3.5$, and $b=2$ fm^{-1} in atomic units $\hbar=m=1$. The 1s, 2p, and 3d cases are described with black line, dashed line, and dot-dashed line, respectively.

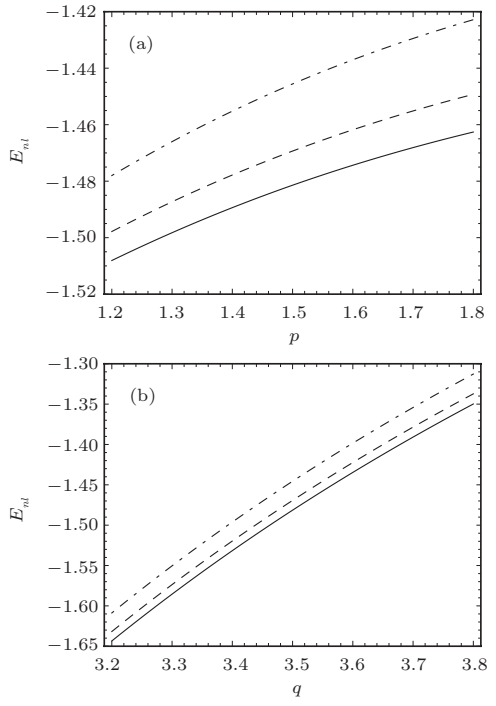


Fig. 2. The effect of parameters p and q on the energy eigenvalues. Figure 2(a) shows E_{nl} varying with p for $A=-5$ fm^{-1}, $B=2$ fm^{-1}, $C=1$ fm^{-1}, $D=1$ fm^{-1}, $q=3.5$, $b=2$ fm^{-1}, and $L=7$ fm. Figure 2(a) displays E_{nl} varying with q for $A=-5$ fm^{-1}, $B=2$ fm^{-1}, $C=1$ fm^{-1}, $D=1$ fm^{-1}, $p=1.5$, $b=2$ fm^{-1}, and $L=7$ fm in atomic units $\hbar=m=1$. The 1s, 2p, and 3d states are described with black line, dashed line, and the dot-dashed line, respectively.

Furthermore, the effects of potential parameters on energy have been explored. The variation E_{nl} with respect to b, L, p, q, A, B, C, and D parameters are presented in Figs. 1–4 for 1s, 2p, and 3d states. It is seen from these figures that the energy values E_{nl} decrease as L, B, and C increase and increase as b, p, q, A, and D increase.

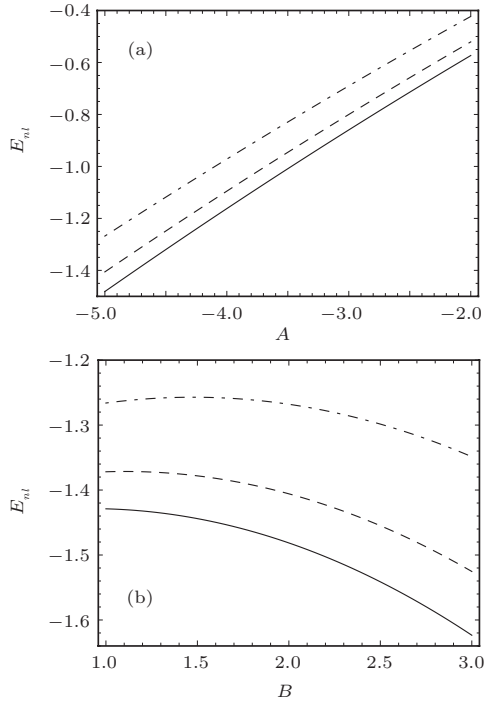


Fig. 3. The effect of parameters A and B on the energy eigenvalues. Figure 3(a) shows E_{nl} varying with A for $B = 2$ fm^{-1}, $C = 1$ fm^{-1}, $D = 1$ fm^{-1}, $p = 1.5$, $q = 3.5$, $b = 2$ fm^{-1}, and $L = 7$ fm. Figure 3(b) displays E_{nl} varying with B for $A = -5$ fm^{-1}, $C = 1$ fm^{-1}, $D = 1$ fm^{-1}, $p = 1.5$, $q = 3.5$, $b = 2$ fm^{-1}, and $L = 7$ fm in atomic units $\hbar = m = 1$. The 1s, 2p, and 3d states are described with black line, dashed line, and the dot-dashed line, respectively.

The graphics given in Fig. 5 shows that how the change the radial bound state wave functions and the radial probability density for different orbitals according to distance from nucleus r. First, we have investigated the relationship between the radial quantum numbers n_r and the radial node points which are defined as points where the electron density is zero. As seen in the figures, the radial wave functions of states 1s, 2p, and 3d have 1, 2, and 3 nodes, respectively and the distances from the nucleus of these node points are different from each other. Another consequence of observed is that the radial wave functions of the bound states are the relationship between amplitudes of the wave function and the corresponding energy. When the energy values of the states in Fig. 5 are compared, it is seen that $E_{10} > E_{21} > E_{32}$ and also one can see in Fig. 5 that there is the similar relationship between the amplitudes of the states as $A_{1s} > A_{2p} > A_{3d}$ (where the A denotes amplitude). On the other hand, we have explored to the radial probability density functions of states. When looking at the graphs on the right side of Fig. 5, it is seen that different peaks are occurred. The largest peak is called the probability density at the maximum away from the nucleus, while the low peaks are defined as the probability densities for the penetration distance. When we compare the graphics in Fig. 5, we see that the maximum distances from the nucleus are $r_{10} = 8,319$ fm (1 fm $= 10^{-15}$ m), $r_{21} = 8656$ fm, and $r_{32} = 8252$ fm for 1s, 2p, and 3d states, respectively.

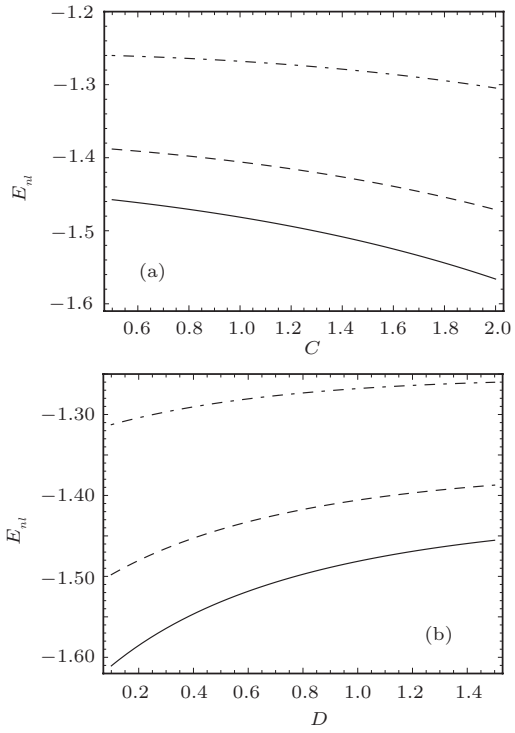


Fig. 4. The effect of parameters C and D on the energy eigenvalues. Figure 4(a) shows E_{nl} varying with C for $A = -5$ fm^{-1}, $B = 2$ fm^{-1}, $D = 1$ fm^{-1}, $p = 1.5$, $q = 3.5$, $b = 2$ fm^{-1}, and $L = 7$ fm. Figure 4(b) displays E_{nl} varying with D for $A = -5$ fm^{-1}, $B = 2$ fm^{-1}, $C = 1$ fm^{-1}, $p = 1.5$, $q = 3.5$, $b = 2$ fm^{-1} and $L = 7$ fm. in atomic units $\hbar = m = 1$. The 1s, 2p and 3d states are described with black line, dashed line, and dot-dashed line, respectively.

Finally, we have studied the special potentials, which are defined in the literature, have been obtained from the multiparameter potential. For these potentials, which are the Manning–Rosen, Hulthen, Eckart-type, Rosen–Morse, Woods–Saxon, Morse, Kratzer–Fues, q-parameter hyperbolic Pöschl–Teller, and Yukawa potentials, the energy eigenvalues for the bound state have been obtained. Also the numerical results have been computed and given in Tables 2–5. In addition to these, to show the accuracy of our results, the numerical energy eigenvalues for these potentials have been compared with the results obtained in previous studies. One can clearly see from Tables 2–4 that the results are in good agreement with other results in the literature.

Surely this paper will be a good reference in the literature due to the fact that the multiparameter potential model describes both core and molecular structures unlike the other potential models. So, the results obtained in this work can be applied to different research areas. For instance, by using the energy eigenvalue formula defined in Eq. (31), one can explore thermodynamic and optical properties of the atoms and molecules.[66–75]

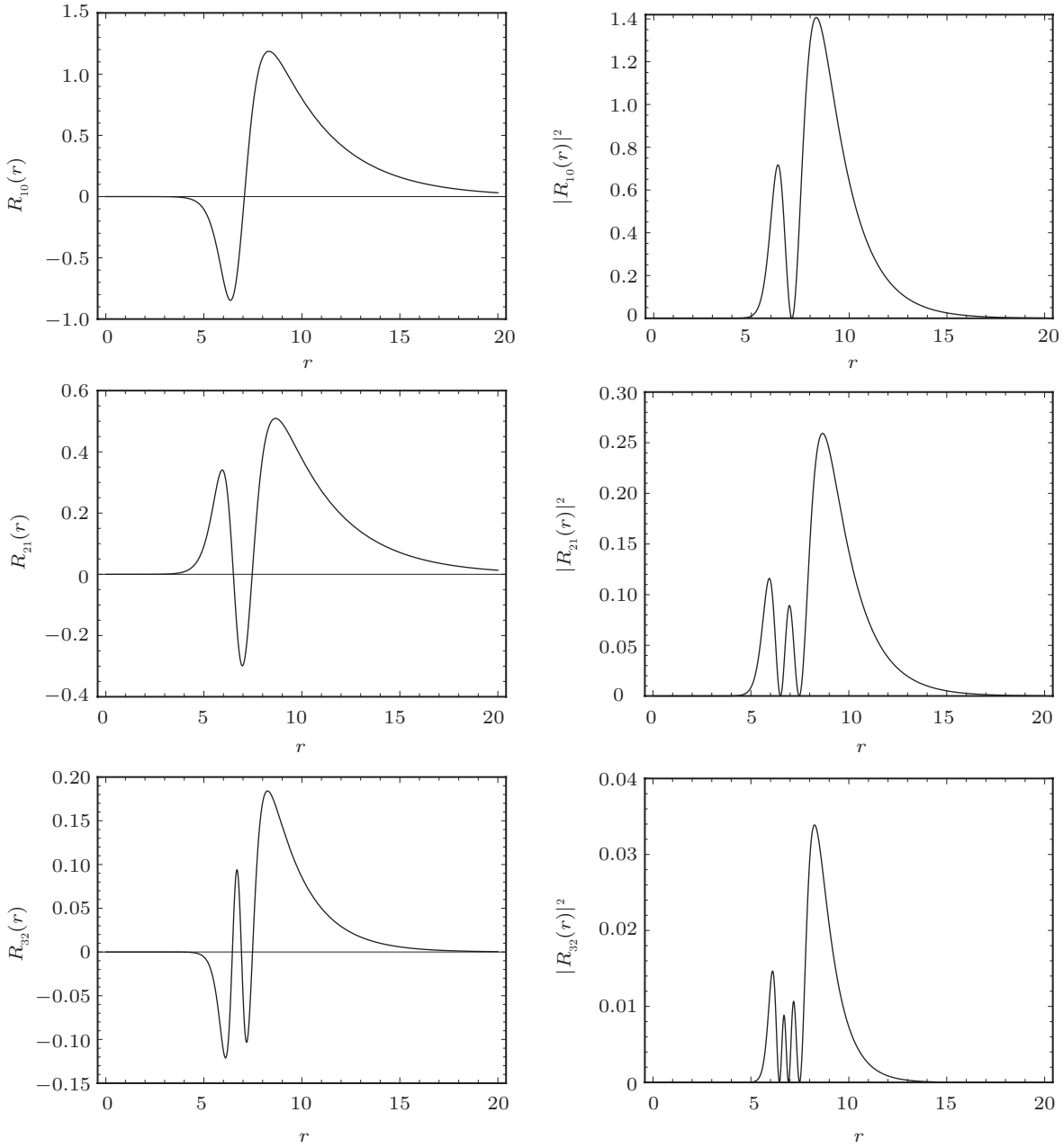


Fig. 5. Variation of the bound states radial wave function and radial probability density with respect to distance from nucleus r for $A = -5$ fm^{-1}, $B = 2$ fm^{-1}, $C = 1$ fm^{-1}, $D = 1$ fm^{-1}, $p = 1.5$, $q = 3.5$, $b = 2$ fm^{-1}, and $L = 7$ fm in atomic units $\hbar = m = 1$. The orbitals energy are $E_{10} = -1.48143$ fm^{-1}, $E_{21} = -1.46934$ fm^{-1}, and $E_{32} = -1.44558$ fm^{-1} for 1s, 2p, and 3d, respectively.

Acknowledgments

The authors wish to thank Hilmi YANAR and referees for helpful suggestions and comments. This work was also supported by Mersin University. The author (Ahmet Taş) wishes to thank for its support.

References

[1] Wang J and Ye W C 2010 *Chin. Phys. B* **19** 030401
[2] Hassan H, Hoda Y B and Lu L L 2012 *Chin. Phys. Lett.* **29** 020303
[3] Taskin F and Kocak G 2010 *Chin. Phys. B* **19** 090314
[4] Lu F L and Chen C Y 2010 *Chin. Phys. B* **19** 100309
[5] Wei G F and Chen W L 2010 *Chin. Phys. B* **19** 090308
[6] Falaye B J, Ikhdair S M, and Hamzavi M 2015 *J. Theor. Appl. Phys.* **9** 151
[7] Xu C L and Zhang M C 2017 *J. Korean Phys. Soc.* **70** 129
[8] Aydogdu O and Yanar H 2015 *Int. J. Quantum Chem.* **115** 529
[9] Abdelmonem M S, Abdel-Hady A and Nasser I 2015 *Int. J. Quantum Chem.* **115**
[10] Gao J and Zhang M C 2016 *Chin. Phys. Lett.* **33** 010303
[11] Yuan Y, Lu F L, Sun D S and Chen C Y 2014 *Commun. Theor. Phys.* **62** 315
[12] Ikot A N and Akpan I O 2012 *Chin. Phys. Lett.* **29** 090302
[13] Ikhdair S M, Falaye B J and Hamzavi M 2013 *Chin. Phys. Lett.* **30** 020305
[14] Wei G F and Chen W L 2014 *Int. J. Quantum Chem.* **114** 1602
[15] Sun G H, Popov D, Camacho-Nieto O and Dong S H 2015 *Chin. Phys. B* **24** 100303
[16] Yazarloo B H, Mehraban H and Hassanabadi H 2016 *Chin. Phys. B* **25** 080302
[17] Pekeris C L 1946 *Phys. Rev.* **70** 518
[18] Greene R L and Aldrich C 1976 *Phys. Rev. A* **14** 2363

[19] Ikot A N, Obong H P, Owate I O, Onyeaju M C and Hassanabadi H 2015 *Adv. High Energy Phys.* **2015** 632603
[20] Jia C S, Chen T and He S 2013 *Phys. Lett. A* **377** 682
[21] Peña J J, García-Martínez J, García-Ravelo J and Morales J 2015 *Int. J. Quantum Chem.* **115** 158
[22] Obong H P, Ikot A N, Owate I O and Hassanabadi H 2016 *New Phys.: Sae Mulli* **66** 2
[23] Onate C A 2015 *Chin. J. Phys.* **53** b1–11
[24] Ikot A N, Hassanabadi H and Abbey T M 2015 *Commun. Theor. Phys.* **64** 637
[25] Ikot A N, Hassanabadi H, Obong H P, Umoren Y C, Isonguyo C N and Yazarloo B H 2014 *Chin. Phys. B* **23** 120303
[26] Zhang G D, Zhou W, Liu J Y, Zhang L H and Jia C S 2014 *Chem. Phys.* **439** 79
[27] Hu X T, Zhang L H and Jia C S 2014 *J. Mol. Spectroscopy* **297** 21
[28] Jia C S, Zhang L H, Hu X T, Tang H M and Liang G C 2015 *J. Mol. Spectroscopy* **311** 69
[29] Onate C A and Ojonubah J O 2015 *J. Theor. Appl. Phys.* 1–6
[30] Alsadi K S 2015 *Appl. Math. Inform. Sci.* **9** 1931
[31] Falaye B J, Oyewumi K J, Ikhdair S M and Hamzavi M 2014 *Phys. Scr.* **89** 115204
[32] Tas A, Alpdogan S and Havare A 2014 *Adv. High Energy Phys.* **2014**
[33] Alpdogan S, Aydogdu O, and Havare A 2013 *J. Phys. A: Math. Theor.* **46** 015301
[34] Sol-Mesa D, Quesne C and Smirnov Y F 1998 *J. Phys. A: Math. Gen.* **31** 321
[35] Simsek M and Yalcin Z 1994 *J. Math. Chem.* **16** 211
[36] Durmus A 2011 *J. Phys. A: Math. Theor.* **44** 155205
[37] Manning M F and Rosen N 1933 *Phys. Rev.* **44** 951
[38] Hulthen L 1942 *Ark. Mat. Astron. Fys. A* **28** 5
[39] Eckart C 1930 *Phys. Rev.* **35** 1303
[40] Rosen M and Morse P M 1932 *Phys. Rev.* **42** 210
[41] Woods D R and Saxon D S 1954 *Phys. Rev.* **95** 577
[42] Morse P M 1929 *Phys. Rev.* **34** 57
[43] Kratzer A 1920 *Zeitschrift fur Physik A: Hadrons and Nuclei* **3** 289
[44] Yanar H, Havare A and Sogut K 2014 *Adv. High Energy Phys.* **2014**
[45] Hamzavi M, Movahedi M, Thylwe K E and Rajabi A A 2012 *Chin. Phys. Lett.* **29** 080302
[46] Ciftci H, Hall R L and Saad N 2003 *J. Phys. A: Math. Gen.* **36** 11807
[47] Ciftci H, Hall R L and Saad N 2005 *J. Phys. A: Math. Gen.* **38** 1147
[48] Yanar H and Havare A 2015 *Adv. High Energy Phys.* **2015**
[49] Aydogdu O and Sever R 2010 *Eur. Phys. J. A* **43** 73
[50] Ovando G, Peña J J and Morales J 2016 *Theor. Chem. Acc.* **35** 1
[51] Falaye B J, Oyewumi K J, Ibrahim T T, Punyasena M A and Onate C A 2013 *Can. J. Phys.* **91** 98
[52] Lucha W and Schöberl F F 1999 *Int. J. Mod. Phys. C* **10** 607
[53] Qiang W C, Li K and Chen W L 2009 *J. Phys. A: Math. Theor.* **42** 205306
[54] Ikhdair S M 2011 arXiv preprint arXiv:1110.3153
[55] Bayrak O, Kocak G and Boztosun I 2006 *J. Phys. A: Math. Gen.* **39** 11521
[56] Ma Z Q and Xu B W 2005 *Europhys. Lett.* **69** 685
[57] Gonul B, Ozer O, Cancelik Y and Kocak M 2000 *Phys. Lett. A* **275** 238
[58] Varshni Y P 1990 *Phys. Rev. A* **41** 4682
[59] Falaye B J 2012 *Central Eur. J. Phys.* **10** 960
[60] Dong S H, Qiang W C, Sun G H and Bezerra V B 2007 *J. Phys. A: Math. Theor.* **40** 10535
[61] Jia C S, Diao Y F, Liu X J, Wang P Q, Liu J Y and Zhang G D 2012 *J. Chem. Phys.* **137** 014101
[62] Zhang G D, Liu J Y, Zhang L H, Zhou W and Jia C S 2012 *Phys. Rev. A* **86** 062510
[63] Wang P Q, Zhang L H, Jia C S and Liu J Y 2012 *J. Mol. Spectroscopy* **274** 5
[64] Yanar H, Aydoğdu O and Saltı M 2016 *Mol. Phys.* **114** 3134
[65] Jia C S, Zhang L H and Peng X L 2017 *Int. J. Quantum Chem.* **117** 14
[66] Jia C S and Jia Y 2017 *Eur. Phys. J. D* **71** 3
[67] Onate C A, Onyeaju M C, Ikot A N, Idiodi J O A and Ojonubah J O 2017 *J. Korean Phys. Soc.* **70** 339
[68] Song X Q, Wang C W and Jia C S 2017 *Chem. Phys. Lett.* **673** 50
[69] Onyeaju M C, Idiodi J O A, Ikot A N, Solaimani M and Hassanabadi H 2016 *Few-Body Systems* **57** 793
[70] Khordad R and Mirhosseini B 2014 *Opt. Spectroscopy* **117** 434
[71] Xiao B, Guo K, Mou S and Zhang Z 2014 *Superlattices and Microstructures* **69** 122
[72] Khordad R and Mirhosseini B 2015 *Pramana* **85** 723
[73] Jia C S, Zhang L H and Wang C W 2017 *Chem. Phys. Lett.* **667** 211
[74] Song X Q, Wang C W and Jia C S 2017 *Chem. Phys. Lett.* **673** 50
[75] Jia C S, Wang C W, Zhang L H, Peng X L, Zeng R and You X T 2017 *Chem. Phys. Lett.* **676** 150